63 3 6

406 704

QUARTERLY TECHNICAL PROGRESS REPORT NO. 2

20 February 1963 through 19 May 1963

P-N JUNCTION FORMATION TECHNIQUES

Aeronautical Systems Division
Air Force Systems Command
Wright-Patterson AFB, Ohio

Contract AF33(657)-10505

ION PHYSICS CORPORATION

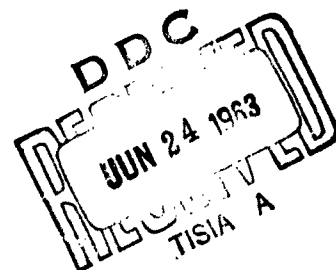Quarterly Technical Progress Report No. 2

20 February 1963 through 19 May 1963

P-N JUNCTION FORMATION TECHNIQUES

Aeronautical Systems Division
Air Force Systems Command
Wright-Patterson AFB, Ohio

Contract AF33(657)-10505

Project Manager _William J. King_

Ion Physics Corporation
Burlington, Massachusetts

NOTICE

The work covered by this report was accomplished under
Air Force Contract AF33(657)-10505, but this report is
being published and distributed prior to Air Force review.
The publication of this report, therefore, does not
constitute approval by the Air Force of the findings or
conclusions contained herein.   It is published for the
exchange and stimulation of ideas.

ABSTRACT

During the second quarter, final tests have been made on all p-on-n cells implanted in the investigation of effects of junction depth on cell performance. Indications are that it will be possible to produce cells having a good match to the solar spectrum by reducing junction depth. Cells with junction depths of 0.76μ have a spectral response peak at 7500 Å (equal energy input) vs. the usual 8500 Å peak for diffusion produced p-on-n-type cells.

Cell efficiency has been raised to the 7-8% range (best cell 8.5%) under 2800°K tungsten illumination. This improvement is apparently due to changes in junction profile.

It has been shown that high oxygen content ($> 10^{15}$ O atoms/cm^3) is an important factor in reducing cell performance. Reflection electron diffraction studies indicate that lattice damage caused by implantation is completely repaired with 800°C annealing for 16 hours. This heat treatment has no effect on bulk lifetime.

Initial investigations on n-on-p cells were made by bombarding 0.4 ohm-cm p-type silicon with phosphorus ions. Results on unfinished cells are analogous to those for p-on-n cells.

OBJECTIVE

The objective of this program is to perform an experimental

and theoretical applied research investigation to

(1)   Increase the efficiency of state-of-the-art p-n
       junction photovoltaic energy converters by ion
       implantation.

(2)   Lower the cell fabrication costs.

(3)   Increase the yield of high efficiency cells from
       each batch.

TABLE OF CONTENTS

ILLUSTRATIONS

TABLES

1. PROGRAM CONSIDERATIONS

The basic considerations and experimental techniques for the ion implantation process were described briefly in Quarterly Report No. 1. Based on these, the program was divided into two main phases:

Phase I

. Investigations of methods of reducing cell series resistance. This involves both contact resistance and sheet resistance.

. Investigations of radiation damage effects including in-process annealing and post-implantation annealing.

. Investigations of cell efficiency as a function of junction depth.

Phase II

. Investigation of cell efficiency as a function of junction profile.

· Investigation of n-on-p type cells.

During the first quarter, cells were implanted with varying parameters to give a sound basis for proceeding to Phase II. All of these cells have now been completely heat treated, contacted and tested and the results of these investigations are presented in this report. In particular, considerable information has been obtained on radiation damage effects and spectral response variations as a function of junction depth. The

latter results indicate the possibility of matching cell response to the solar spectrum and additional junction depth variation studies are therefore being performed as part of the drift field study.

The special implantation chamber for controlling junction profiles in the Phase II studies is now complete and drift field effects are being studied. Preliminary results show some improvement in conversion efficiency with a 10:1 concentration gradient (surface-to-junction) vs. a "flat" profile. Interpretation of this result is difficult since other factors such as radiation damage and material variations were quite important in these runs. Investigations from now until contract termination will primarily study drift field effects and the interrelation of drift field and junction depth.

The following sections discuss junction depth effects, drift field effects, and radiation damage effects. No further direct work has been performed on series resistance effects but preliminary investigations were made on n-on-p-type cells.

2. JUNCTION DEPTH EFFECTS

2.1 RANGE-ENERGY RELATIONSHIP

A significant part of the junction depth study has involved a determination of the range-energy relationship for B^{11} ions in silicon. The effective range for device fabrication was determined by measuring junction depth of ion implanted cells using the angle-sectioning technique described in the first quarterly report. Additional data have been obtained and are presented in Fig. 1. This shows an extrapolation of Northcliffe's [1] data for B^{11} in Al at higher energies converted to B^{11} in Si using the Bragg-Kleeman relation:

$$\frac{R_{Si}}{R_{Al}} = \frac{\rho_{Al}}{\rho_{Si}} \frac{\sqrt{A_{Si}}}{\sqrt{A_{Al}}} \tag{1}$$

where R_{Si} and R_{Al} $\equiv$ ranges in Si and Al respectively

ρ_{Si} and ρ_{Al} $\equiv$ densities of Si and Al respectively

A_{Si} and A_{Al} $\equiv$ atomic weights of Si and Al respectively

The circles represent experimental IPC data for which a maximum error of $\pm 0.1\mu$ may be assumed. The three higher energy points were obtained from cells in which the maximum penetration depth corresponded to an angle of incidence of 90° at the particular energy.
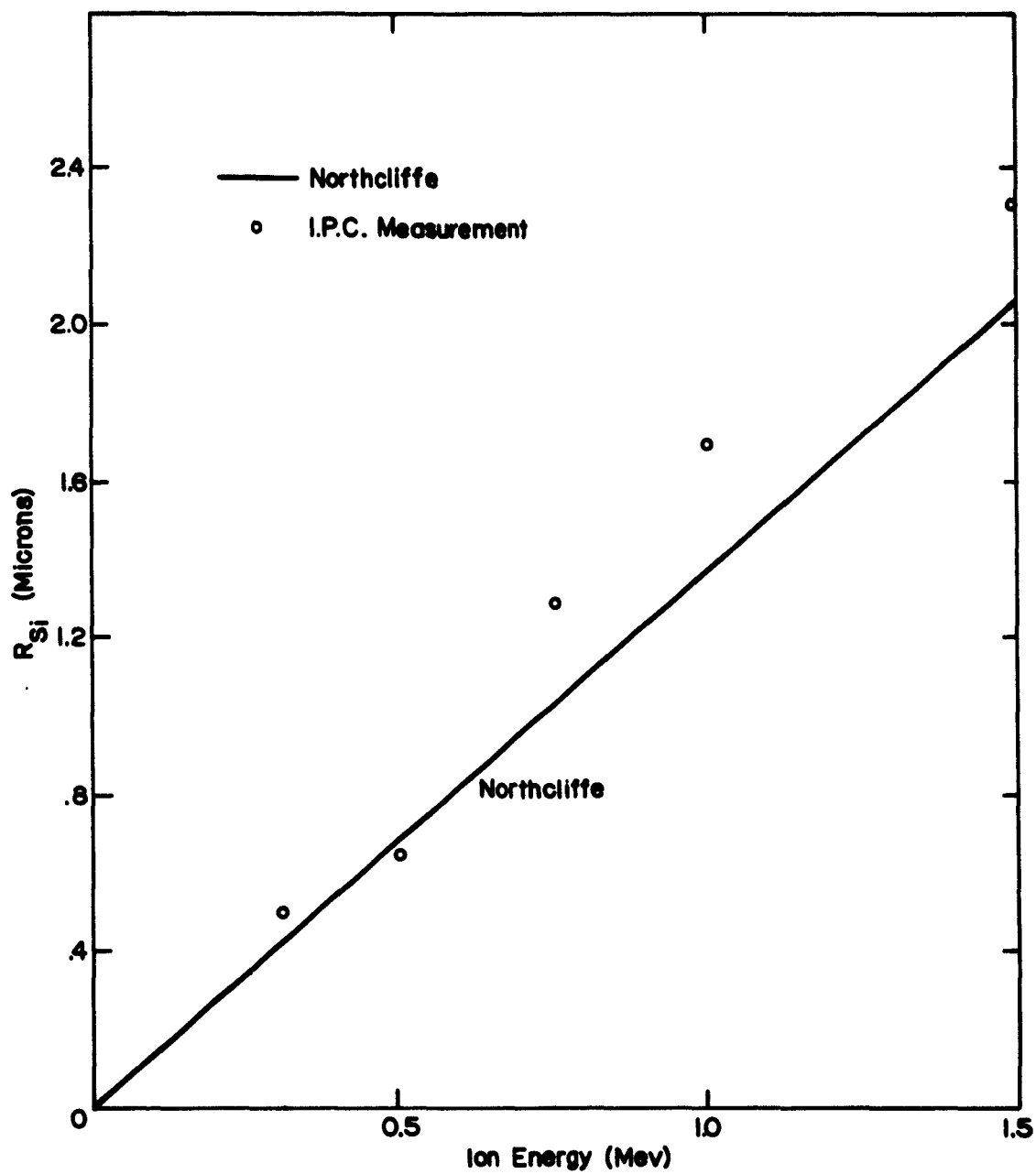
Fig. I RANGE B" IONS IN SILICON

Due to some difficulty in obtaining sufficient beam current at low energies, shallower junction cells were implanted by using a 1 Mev beam at smaller incident angles. The maximum penetration depths for the two lower energies therefore correspond to the maximum angle of incidence used; viz.,

$$R_{max} = R_{90°} \sin \theta_{max} \qquad (2)$$

where R_{max} = maximum penetration depth
normal to cell surface

$R_{90°}$ = range at 90° angle of incidence

θ_{max} = maximum angle of incidence

Since the range may be a function of the apparent linear density of atoms as a function of incident angle, the lower energy points are open to some question. Modifications have been made in the accelerator which now permit "direct" implantations at energies down to 100 Kev. Although cells have been implanted at energies as low as 200 Kev, angle sections to determine junction depth are not yet available.

The IPC data agrees roughly with the Northcliffe extrapolation with a tendency to give ranges approximately 12% greater (except for point at 500 Kev). Both sets of data are consistent within 10% with interpreted values for B^{11} in Si from Powers' and Whalings' data.[2]

The experimental IPC curve is more than adequate for controlling the characteristics of devices formed by ion implantation. As more data are acquired at low energies, still better control of characteristics will be obtained.

2.2   CHARACTERISTIC MEASUREMENTS

2.2.1   Solar Simulator

A delay has occurred in delivery of the Spectrolab Model D-1203 solar simulator which is to be used for measuring cell efficiencies under solar irradiation. Until delivery, cell efficiencies are being measured under 2800°K tungsten light. In addition to the small projection lamp apparatus described in the first quarterly report (Section 6.1), a 2-kilowatt lamp is being used to measure efficiencies at incident fluxes up to 140 mw/cm^2. This lamp is water-cooled and voltage-stabilized and gives consistent results with careful positioning of the cell being tested. As described below, relative cell response under solar illumination may be calculated from the light source spectra and cell spectral response curves. The applicability of this technique may be studied when the solar simulator is operable.

2.2.2   Efficiency Measurements

Efficiency measurements on all cells implanted in the junction depth study have been completed. These cells have junction depths ranging from 0.76µ to 2.54µ after heat treatment and have efficiencies of 4.5 → 6.0%. All efficiency measurements are now being conducted at 140, 120, 100, 80 and 60 mw/cm^2 incident radiation. Figure 2 shows the response curves for a typical cell produced during the first phase of the program. This cell has a junction depth of 0.89µ and shows linear response as a function of incident intensity. The curves are normally obtained by masking off a 1 x 1 cm area in the center of the circular cells and then multiplying the resulting currents by 2 for comparison with conventional 1 x 2 cm cells.
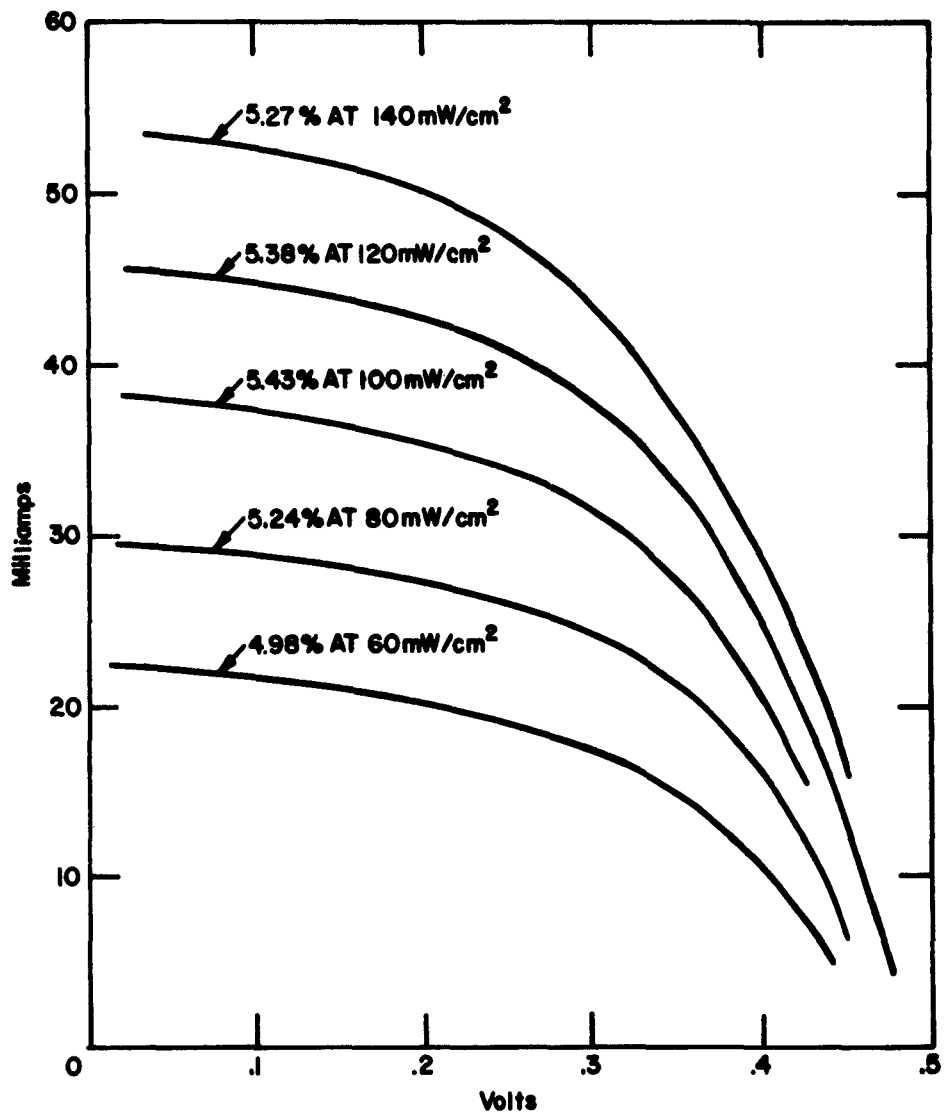
CELL D-57

FIG. 2   EFFICIENCY   MEASUREMENT AT INTENSITIES OF 60,80,
100, 120 & 140 mW/cm² (2800°TUNGSTEN)

I-259

7

The impurity distribution in all of these cells was nominally flat from cell surface to junction. In practice, due to experimental difficulties, the profile was flat in the middle with a slight drop-off in concentration at the junction and a sharp drop-off near the surface. The latter represents a reverse drift field tending to reduce collection efficiency. The experimental problems were overcome with the sample rotator described in Section 3 and cells subsequently fabricated with concentration gradients of 10:1 (surface-to-junction) had efficiencies as high as 8.5%.

When tested with an unfiltered tungsten source, there is no apparent variation of efficiency with junction depth. This lack of change is almost certainly due to a conflict of factors; i.e., improved collection efficiency vs. poorer spectral match (see below) with test light source as depth is decreased. As the junction depth is decreased, collection efficiency increases since more carriers are generated in the bulk region where lifetime is high. The match of the spectral response curve to the illuminating light (tungsten), however, gets worse and the two changes tend to cancel each other.

2.2.3   Spectral Response

Figure 3 shows the marked progression in spectral response towards the blue as junction depth is decreased. No "finished" cells have been made with junction depths less than 0.76μ, however, such cells will be made as part of the current drift field study. An additional shift can be expected in these cells. For comparison purposes, the response for the shallowest cell has been replotted in Fig. 4 for equal energy input at each wavelength and is seen to peak at ~ 7500 Å.
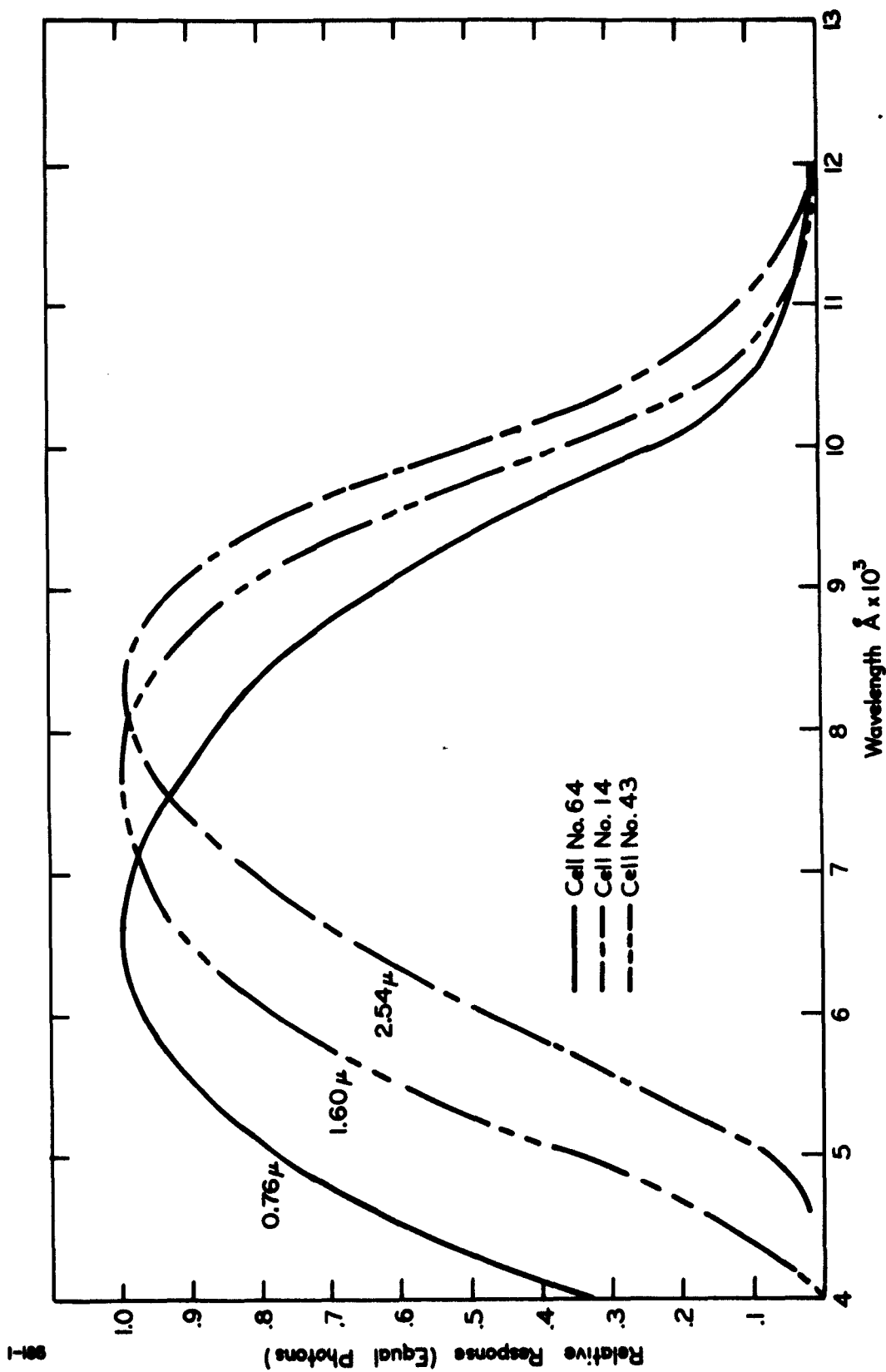
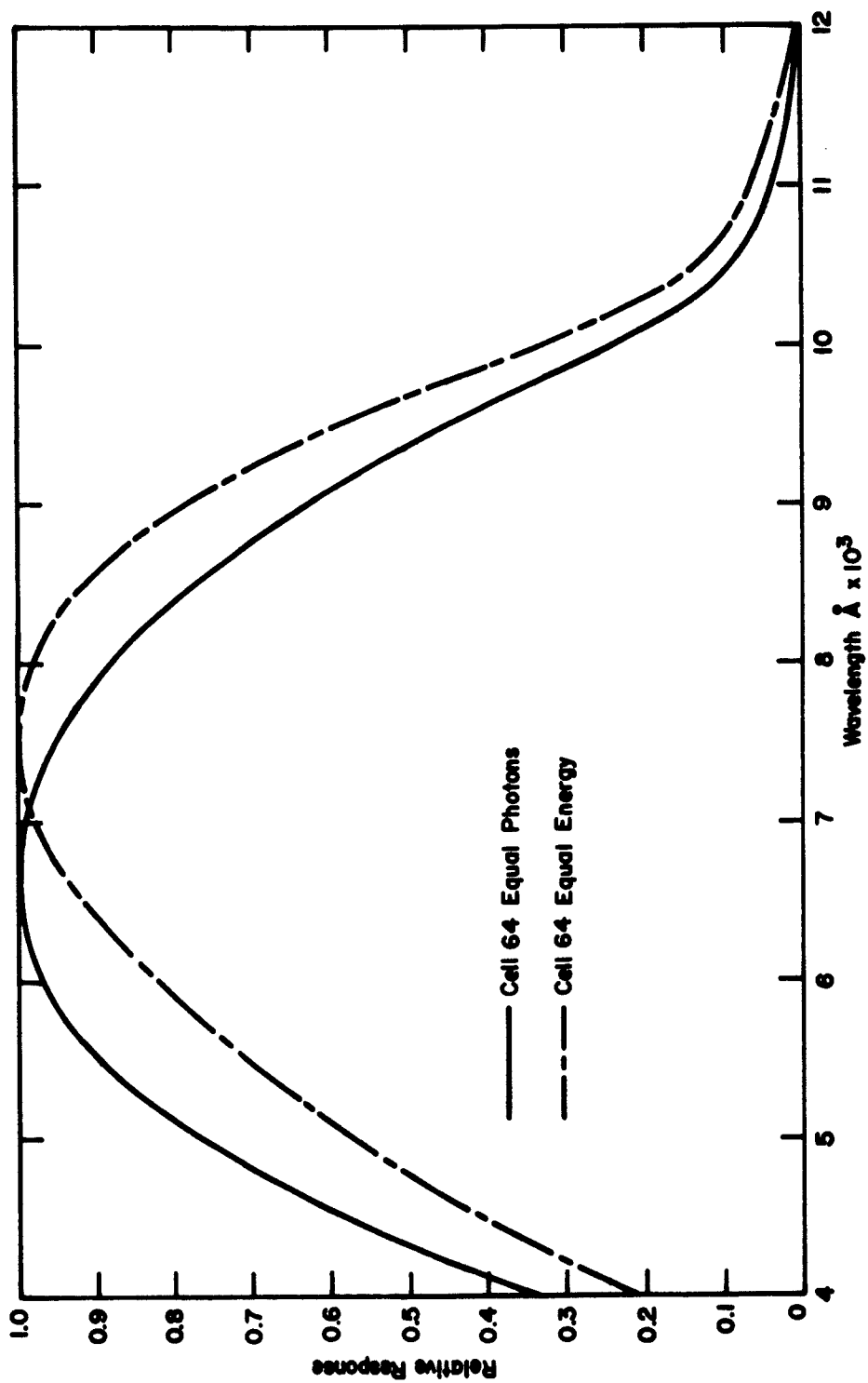FIG. 3 SPECTRAL RESPONSE OF I.P.C. CELLS

FIG. 4   SPECTRAL RESPONSE

From Fig. 3 it is apparent that the shallower junction cells have a much wider response than the deep junction cells. This occurs because additional blue response is obtained with the shallower junction while most of the red response is retained because of the higher lifetime in the bulk region.

A continuation of the "blue shift" with shallower junctions would lead to cells with superior response under "solar" illumination. This is evident from Fig. 5 which gives the response of an IPC cell with a junction depth of 0.76μ, a diffusion-produced cell (IRC standard #77) and the relative radiance curves of a tungsten light (2800°K) and the sun (N. R. L.). These normalized curves may be multiplied point-by-point to obtain the product curves

(1)   IPC x Tungsten

(2)   IPC x Solar

(3)   IRC standard x Tungsten

(4)   IRC standard x Solar

as shown in Fig. 6 (ends of curves removed for reproduction). The relative areas under these curves and the decrease in response when solar light is used rather than tungsten light are given in Table I.

Table I - Solar vs. Tungsten Response

	Solar Illumination	2800°K Tungsten Illumination	Tungsten-to-Solar Decrease
IPC #64	1568	1665	~ 6%
IRC Standard #77	1232	1764	~30%
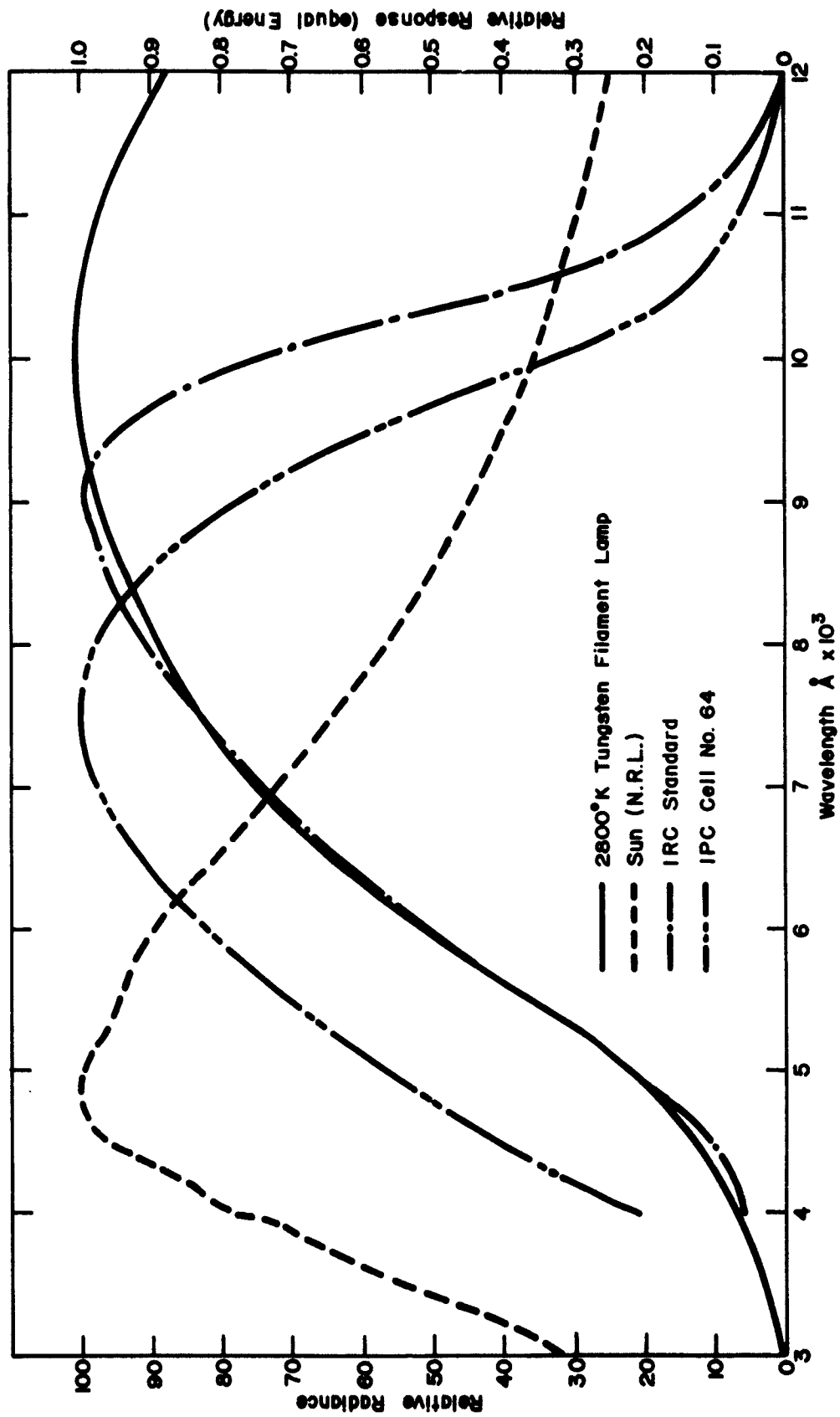
FIG. 5 COMPARISON OF SPECTRAL RESPONSE AND RELATIVE RADIANCE

Relative Response (equal Energy)

Relative Radiance

Wavelength Å x10³

2800°K Tungsten Filament Lamp
Sun (N.R.L.)
IRC Standard
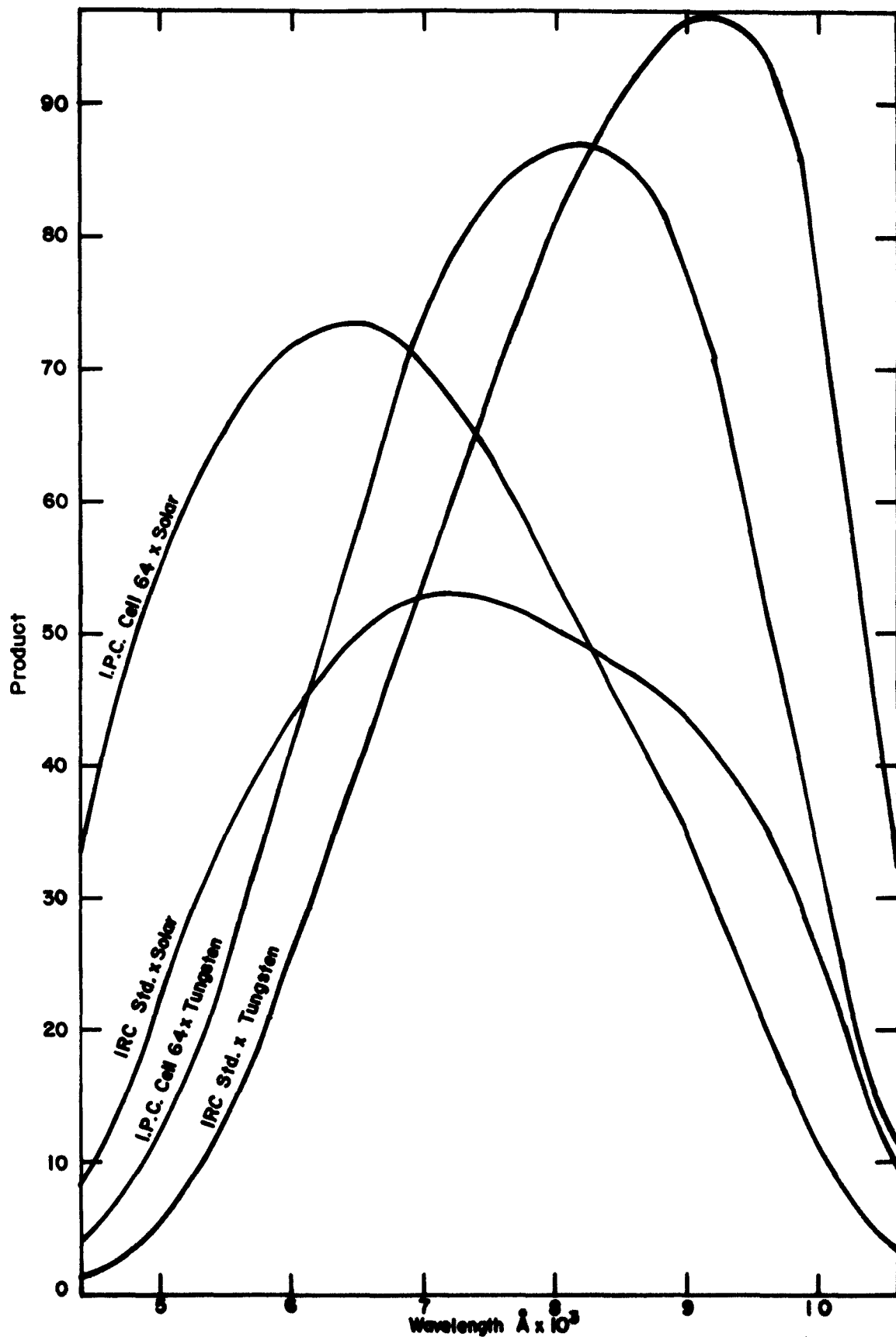IPC Cell No. 64

1-266

12

FIG. 6 PRODUCTS OF EQUAL ENERGY SPECTRAL RESPONSE
TIMES RADIANCE (N.R.L. SOLAR, 2800°K TUNGSTEN)

1-264

From these calculations it is expected that the standard cell would degrade considerably more under solar illumination than the shallow junction IPC cell. A direct comparison can be made when the solar simulator is delivered.

The expected degradation of the IRC standard cell under solar illumination is consistent with empirical results of tests by Hoffman Electronics Corporation.[3] These tests show an average degradation of 21% for p^+-on-n cells with an average peak response of 0.862μ. Considerably greater degradations (up to 33%) were found for high efficiency cells (14% tungsten) than for low efficiency cells (9% tungsten). In general, their tests indicate that the very high efficiencies obtained with some cells is primarily due to better spectral match to a "tungsten" test light and does not indicate the same degree of improvement under solar illumination. Considerable care in measuring cell characteristics is therefore required.

Preliminary results on ion implanted cells with drift fields (see Section 3), combined with the above results on the blue shift with decreased junction depth, indicate the possibility of producing cells with increased efficiency under solar rather than tungsten light. More data on cells with greatly reduced junction depths ($<0.3\mu$) will be available shortly.

3. DRIFT FIELD EFFECTS

3.1   SAMPLE ROTATOR SYSTEM

During this quarter the new sample irradiation system was placed in operation.   The system consists basically of a sample holder which is rotated in the beam to obtain a continuous implantation of ions from cell surface to junction.   The general implantation technique was described in the first quarterly report.

Figure 7 shows the basic features of the system which is constructed entirely of stainless steel to avoid contamination from sputtered ions. Samples are mounted on a holder which may be heated or cooled to obtain implantation temperatures from 800°C to -195°C. The cold system is shown in the diagram; a small change in the holder is required for heating. A retractable beam-viewing glass is incorporated so the profile of the irradiating beam can be observed while adjustments are made   on the beam scanner and other beam-controlling systems until the desired uniform irradiating area is obtained. This viewer is inserted directly in front of the sample and therefore the beam size and uniformity at the sample can be controlled quite accurately.

Since the incident flux varies as a function of incident angle, a control must be provided to program the position of the sample as a function of time. Basically, this controls the speed of rotation at any given angular position of the sample and therefore the integrated flux at that angle. Variations in the program permit variations in the doping profile.
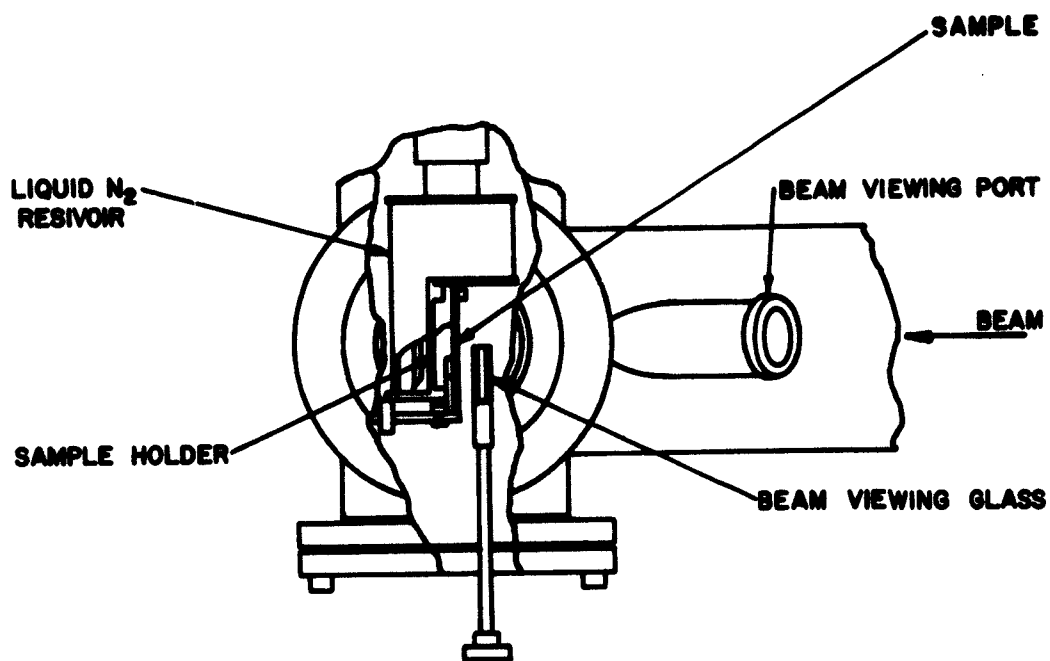
SAMPLE

LIQUID N₂
RESIVOIR

BEAM VIEWING PORT

BEAM

SAMPLE HOLDER

BEAM VIEWING GLASS

FIG. 7   SAMPLE ROTATOR

16

The necessary control is obtained by connecting the drive shaft of the sample holder to a position servomotor which is controlled by a Vernistat adjustable function generator. The latter consists basically of an autotransformer with 101 output taps at 1% increments. There are 34 sliders, each of which may be separately connected to any of the 101 output voltages. A continuously variable resistance is sequentially connected between adjacent sliders by a commutator and is used to advance linearly from one slider voltage to the next. The output from the Vernistat therefore consists of 33 straight line segments. The resistance element is a 3-tap interpolator such that 2 taps are always in contact with 2 of the sliders. Switching between sliders is therefore smooth and non-critical. An output wiper is synchronized with the switching operation so that it is always wiping on an energized portion of the interpolating resistance element.

The necessary drive voltage for the position servo is applied to the input of the Vernistat and the 34 sliders are adjusted to give the necessary function. The position of each of the sliders determines the voltage level applied to the position servo when the interpolator reaches that position and therefore determines the position of the sample holder. A d.c. motor is used to move the output interpolator contact along the function. By variations in the positions of the sliders an almost unlimited variety of doping profiles may be obtained. In addition, by varying the speed of the d.c. motor, the total time to cover the function (i.e., to rotate the sample through the required angle) may be controlled to determine doping level. The system therefore affords complete control of doping profile and doping level in the samples. Figure 8 shows a photograph of the entire system composed of the sample irradiation chamber, position servomotor (black box on top of chamber) and the Vernistat control and associated electronics.
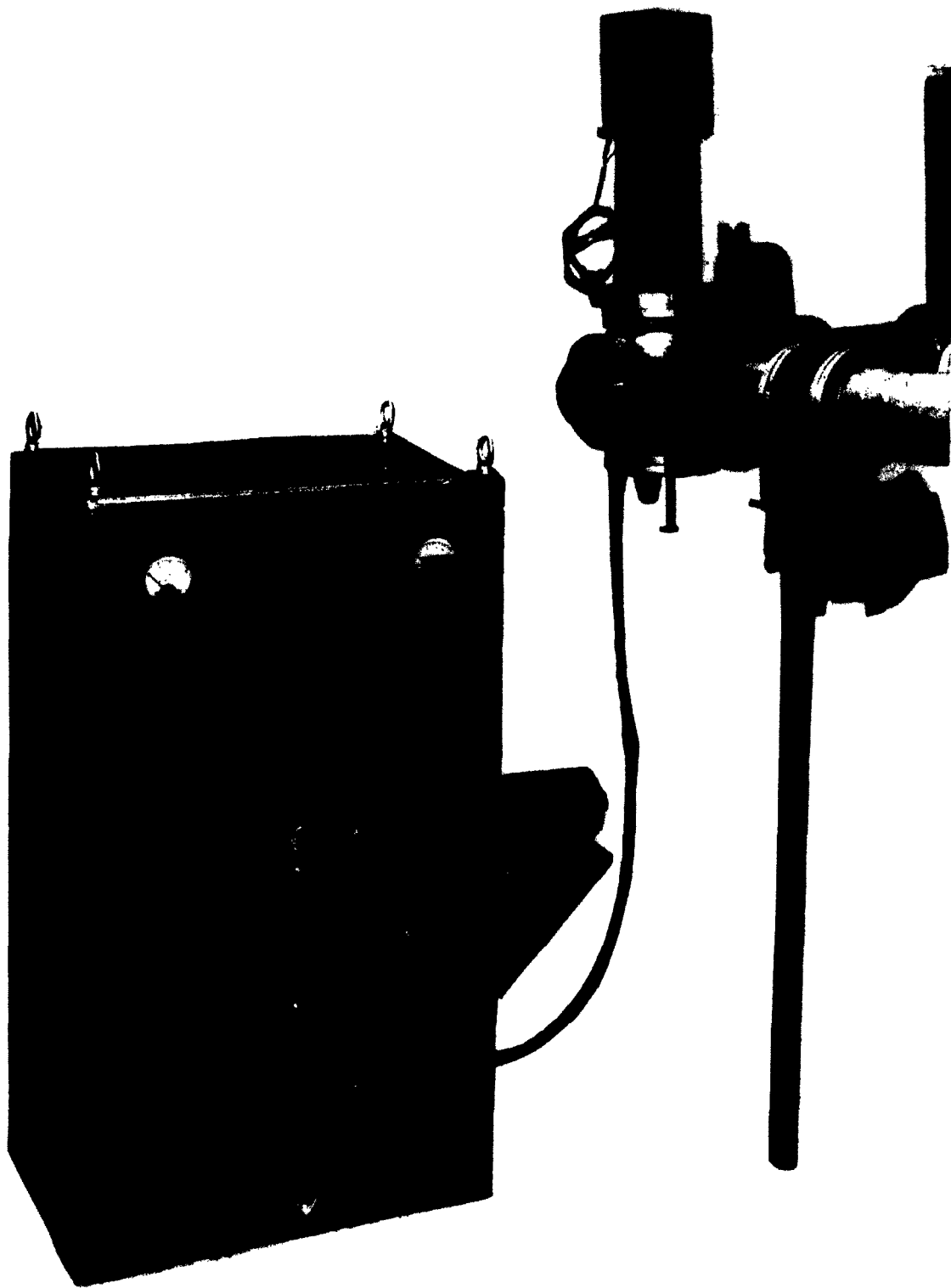
FIG. 8 SAMPLE CHAMBER AND ROTATING SYSTEM

The actual position of the sample as a function of time is monitored continuously. Operation of the system, as shown by this monitoring, is completely satisfactory. Deviations from the desired profile due to factors such as drift in the d.c. motor speed are estimated at less than 5%. The system is now being used in the profile study and will shortly be used in an investigation of radiation damage effects during low temperature implantation.

3.2 PROFILE STUDIES

For initial investigations on drift field effects in the surface region, a program was set up in which cells were to be fabricated with flat, 10:1 (surface-to-junction) linear and 100:1 linear concentration profiles. The implanted concentrations were arbitrarily set at approximately 10^{19} B^{11} atoms/cm^3 for flat, 5×10^{19} at surface to 5×10^{18} at junction for 10:1, and 10^{20} at surface to 10^{18} at junction for 100:1 profiles. The average concentration was therefore approximately 10^{19} B^{11} atoms/cm^3 in each case. The junction depth was to be varied over the range from 0.14μ to 1μ to investigate the interrelation of spectral response effects (see Section 2.3) and drift field effects. For reference, the field for a linear concentration gradient of 100:1 and a 0.25μ junction depth would be $> 2,000$ volts/cm at the cell surface. This should be adequate to demonstrate the effect of drift fields for enhancing collection efficiency in the surface region.

An unfortunate initial choice was made for the material to be used in this investigation. Previous investigations had shown that comparable cells were obtained with float zoned or pulled n-type crystals if the material were relatively oxygen-free ($< 10^{15}$/cm^3), had adequate lifetime (>10 μsec), and had resistivity of approximately 0.4 ohm-cm. In order to avoid the masking procedure necessary for directly measuring efficiency of a 1 x 1 cm area from a circular sample, precut 1 x 2 cm

blanks with the above characteristics were ordered from a new manu-
facturer. This material was used at the beginning of the drift field study
and for an extended period very inconsistent results were obtained and
cell efficiencies were markedly lower than previous values.

Although the results were of little value in studying drift field
effects, they did point up an important factor in making cells by implan-
tation techniques. When the difficulty was traced to material problems,
the oxygen content of various cells was checked. It was definitely estab-
lished (see Section 4) that all of the higher efficiency cells had been made
from relatively oxygen-free material and, in fact, the best cells were
made from float zoned material which is known to have the lowest oxygen
concentration. Re-examination of the older data also indicated a definite
trend to better cells if the implanted layer were parallel to the (111) plane.
Based on these results and other data, preferred material would have
the following characteristics:

(a) oxygen free - $10^{15}/cm^3$ or less, as low as attainable

(b) (111) orientation

(c) high lifetime - 20 μsec or greater, consistent with
     low bulk resistance

(u) float zoned

Low dislocation density would also be desirable but is incon-
sistent with float zoned material. Because of the importance of oxygen
content, float zoned material with the above characteristics will be used
in future investigations.

After the material problem was discovered, the drift field program was started again using float zoned material used in the junction depth study. Only cells with 10 : 1 profiles have been finished so far. Figure 9 shows the I-V curves for one of the 10 : 1 profile cells. Although complete measurements on these cells are not yet available, the definite improvement in efficiency over the Phase I cells is obvious. This cell was implanted at 750 Kev and had a peak spectral response at ~ 7800 Å (equal photons) in close agreement with the 750 Kev flat profile cells. If the same spectral response shift is observed in these cells as occurred in the flat profile cells, the ion-implanted cells may shortly be competitive with diffusion produced cells under solar illumination. Considerably more experimental data, particularly under solar illumination, is required before definite predictions can be made. Better material has been ordered, conforming to the above specifications, and will shortly be used to extend the profile investigation to higher drift field configurations.
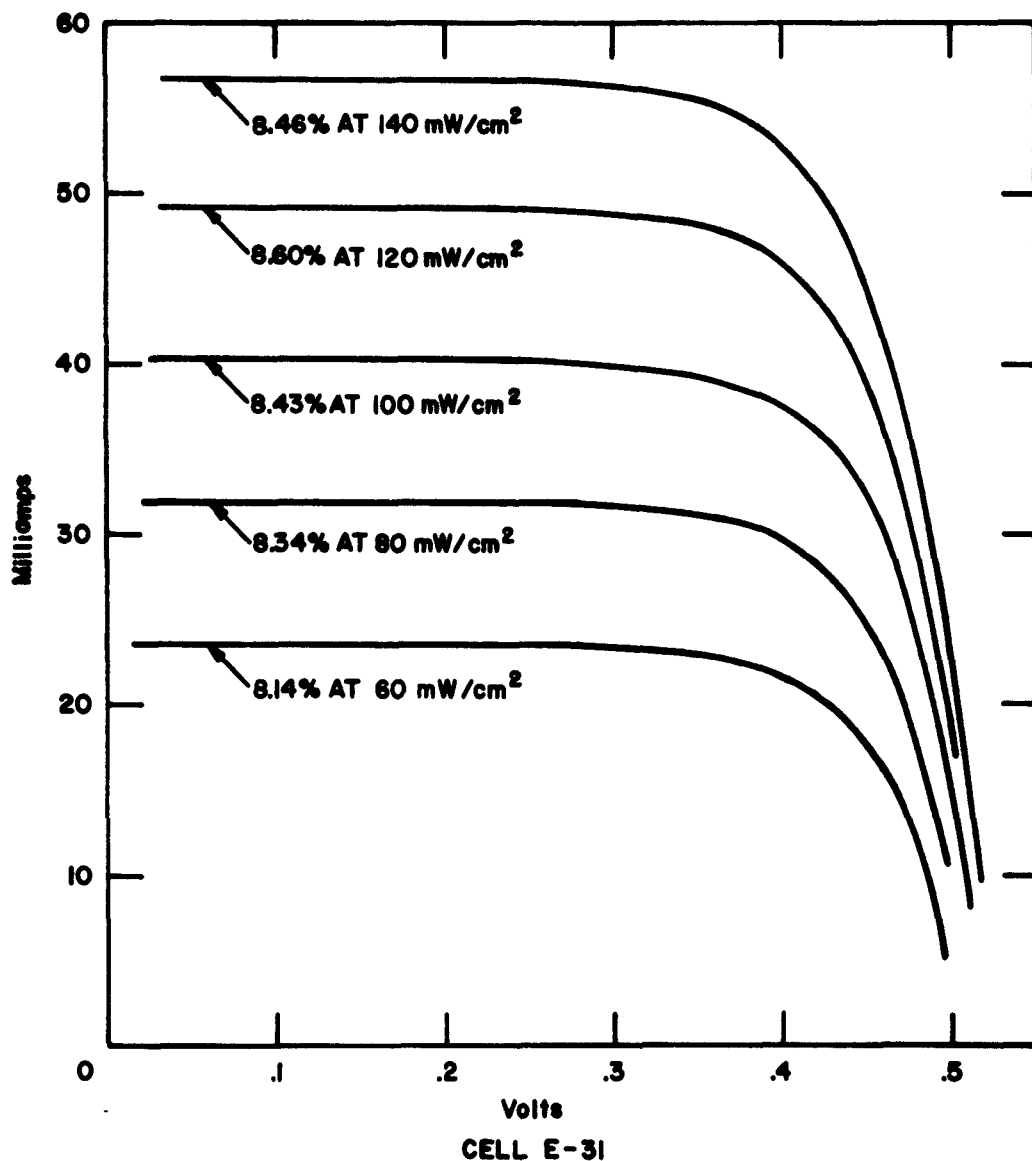
FIG. 9 EFFICIENCY MEASUREMENT AT INTESITIES OF 60, 80,100,
120 & 140 mW/cm² (2800°TUNGSTEN)

22

4. HEAT TREATMENT AND RADIATION DAMAGE EFFECTS

In the first quarterly, a brief discussion of the radiation damage mechanism was given and preliminary results on annealing effects were discussed. Additional data obtained concerning annealing temperatures, carrier lifetimes and radiation damage effects give some insight into the mechanism of junction formation by ion implantation.

4.1 JUNCTION DEPTH VS. HEAT TREATMENT

The angle sectioning technique has been used to determine the effect of annealing temperatures on junction depth. Each of a series of samples (junction depths 0.5 μ to 2.3 μ) was sliced into two pieces yielding a control group and a study group. The latter were heat-treated at 800°C in an argon atmosphere for 16 hours. The results of junction depth measurements on these two groups are given in Table II from which it is evident that heat-treated samples invariably have deeper junctions.

Table II - Predicted vs. Actual Junction Depths

Predicted (Northcliffe Data)	Non-Heat-Treated	Heat-Treated
2.15 μ	2.29 μ	2.54 μ
1.43	1.68	2.08
1.07	1.27	1.60
0.71	0.64	0.89
0.50	0.51	0.76

Within experimental accuracy of $\pm 0.1 \mu$, the magnitude of junction movement is the same for all cells. This indicates a mechanism related to the implantation technique and effective $\sim 0.25 \mu$ past the deepest implanted ions.

An attempt was made to isolate the mechanism by performing a multiple heat treatment on one sample. This sample was sectioned into three pieces which were subsequently heat-treated at different temperatures. A piece treated at 400°C for 64 hours had a junction depth of $1.1 \pm 0.1 \mu$, the same as the non-heat-treated piece. The third piece had a junction depth of $1.5 \pm 0.1 \mu$ after heat treatment at 800°C for 16 hours. Subsequent heat treatment of the 400°C piece at 800°C for only 45 minutes increased the junction depth also to $1.5 \pm 0.1 \mu$. Although temperatures in the 800°C range are required to cause the junction shift, the process involved is not ordinary diffusion since the effect is time-independent after the initial movement.

Since there is a continuous increase in efficiency as the heat treatment is carried out at successively higher temperatures up to the limiting value of ~ 800°C, two effects are occurring. Some of the boron ions during implantation are going directly into lattice positions as shown by the junction before heat treatment, but enough radiation damage exists to "kill" the photo response. Heat treatment at 350°C removes much of the radiation damage (see Section 4, First Quarterly Report) but does not put any more boron into lattice positions. A small increase in photo response is observed due to restoration of the lattice. Heat treatment at 800°C then supplies the activation energy required to put more boron atoms into lattice positions and a much improved photo response is observed. Two activation energies appear to be involved in the process; the first for removal of

radiation damage and the second for transferring boron atoms from interstitial to electrically active lattice positions. However, as evident from the results in the following sections, both of these processes are considerably more complicated than this simple explanation.

There has been some work on radiation enhanced diffusion[4] which indicates that this may be the primary mechanism involved in junction movement. This work reported an increase in the diffusion coefficient for impurities in silicon in areas irradiated with energetic protons (250 Kev to 1 Mev). This phenomenon has a threshold of approximately 750°C and occurs at the end point of the proton range. It is tempting to associate this mechanism with the results above except that a lifetime of 130 sec. was reported for the defects causing the motion. Since the diffusion was carried out at the same time as the bombardment in these experiments, in-process annealing must certainly have occurred. It seems likely that the defect lifetime actually represented an equilibrium condition between defect formation and annealing. In the present work, annealing is carried out sometime after the sample has been bombarded and the defects responsible for the enhanced diffusion could be piling up during irradiation. Further work in this area is obviously required to determine the applicability of this mechanism to the present investigation. In particular, if the effect is occurring it is necessary to determine if it can be avoided while supplying the activation energy required to place boron atoms in lattice positions. Since the threshold temperature for both effects is between 750°C and 800°C, a separation of the two will be very difficult. However, the movement is of small magnitude in any case and is accurately predictable. The proposed advantage of the ion implantation for controlling junction profile therefore appears to be unaffected.

4.2 CARRIER LIFETIME VS. ANNEALING TEMPERATURE

The carrier lifetimes of the bulk material of several of our samples have been measured using a microwave technique. The results of these measurements indicate a variation of $5\,\mu$sec in the raw material obtained from different manufacturers (specifications called for $10\,\mu$sec) from $10\,\mu$sec to $15\,\mu$sec. This difference was noticeable as a red shift in some of the cells.

It was definitely confirmed that the lifetime of the bulk material is completely unaffected by the $800°C$ temperature used for damage annealing. Material which had $10\,\mu$sec lifetime when purchased still had a lifetime of $10\,\mu$sec after undergoing the complete cell fabrication procedure. Starting material of higher lifetime would therefore yield more efficient cells and $20\,\mu$sec material has been ordered for future investigations. The resistivity specification had to be relaxed to 1 - 5 ohm-cm in place of 0.4 ohm-cm to obtain higher lifetime but this is expected to have little or no effect on cell characteristics.

4.3 OXYGEN EFFECTS

At the beginning of the drift field program (see Section 3.2) cells were fabricated which showed a marked efficiency loss when compared to earlier cells. Since these cells were fabricated from pulled crystal slices, high oxygen content was suspected and a comparison of oxygen content in good and bad cells was made.[*] The measurements were made on a Perkin Elmer Model 221 diffraction grating spectrometer. Figure 10 shows part of the infrared spectra of typical silicon slices from Manufacturer A. The three curves represent the blanks as delivered,

---

[*] These measurements were made at the Massachusetts Institute of Technology, Lincoln Laboratories, through Dr. E. P. Warekois.
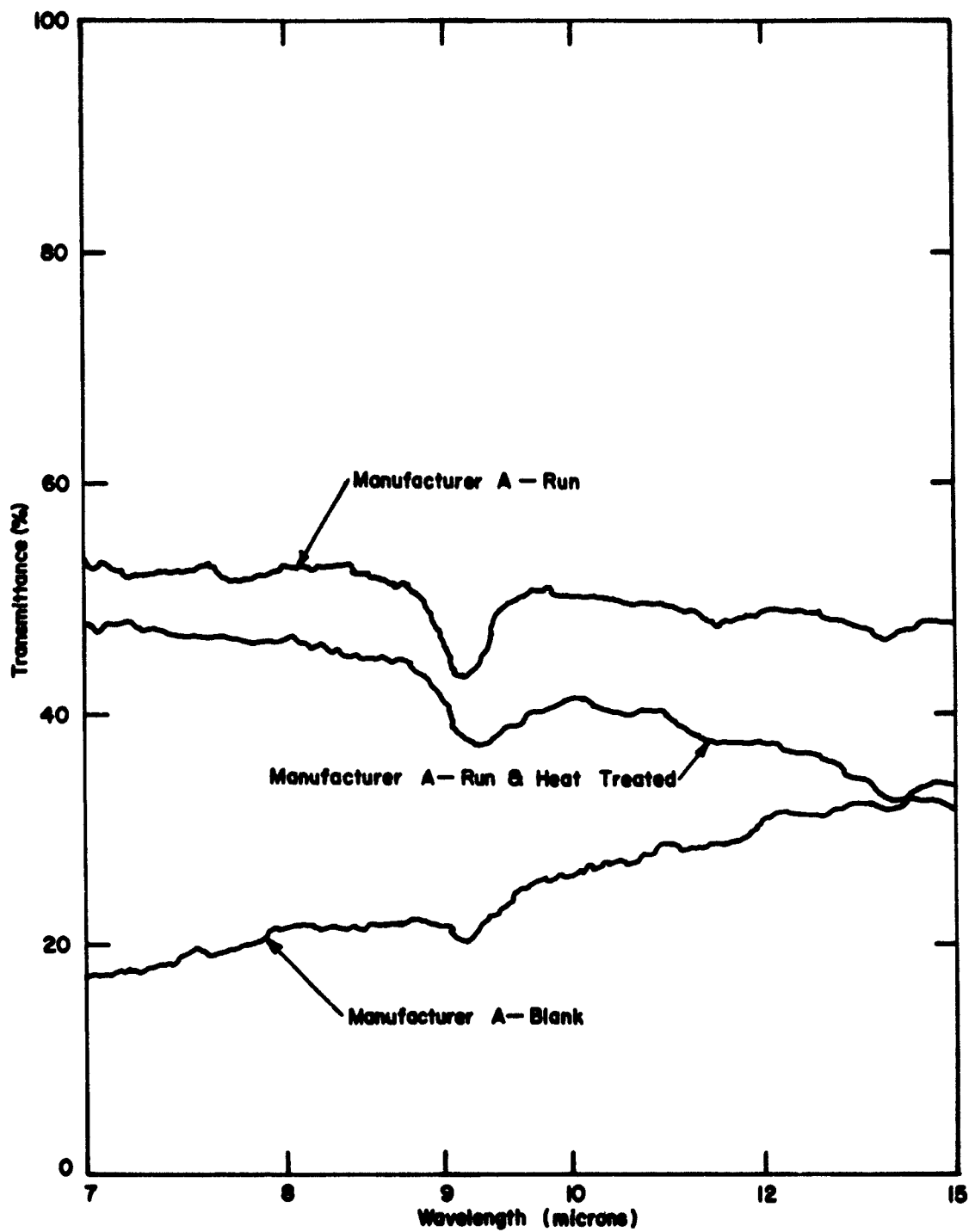
FIG. 10 INFRARED MEASUREMENTS

I-285

27

implanted cells and implanted and heat-treated cells, the latter two having polished surfaces. Cells from this supplier invariably had very poor conversion efficiencies. The peak at 9μ corresponds to the oxygen peak in silicon and is present at all stages in the process. A high background with a reverse slope was obtained with the lapped surface blank. This was caused by light scattering from the surface and tended to wipe out the oxygen peak. No significance is therefore attached to the smaller peak height; i.e., since a spectroscopically pure beam was used, it is certain that oxygen was not introduced into the crystal bulk during implantation.

The latter point was definitely established when polished samples from Manufacturers B and C (Fig. 11) were run and gave no indication of an oxygen peak. Slices from B were also from a pulled crystal while those from C were float zoned material. Specifications for all three manufacturers called for less than 10^{15} O atoms/cm^3. Although some medium efficiency cells have been made with the pulled crystal material from B, the best cells invariably have been made with the float zoned material.

Although no difference can be established between the oxygen content of the material from B and C, float zoned material, as determined by more sensitive measurements, normally has lower oxygen content. Oxygen content in cells produced by implantation methods is therefore a very important parameter. It is difficult to determine content exactly without a standard specimen for comparison but an estimate for crystal A of $>10^{17}$ O atoms/cm^3 has been made by interpolating from the values given by Kaiser, et al,[5] for various values of α_o (α_o = absorption coefficient due to oxygen and is approximately 3.9 for crystal A).
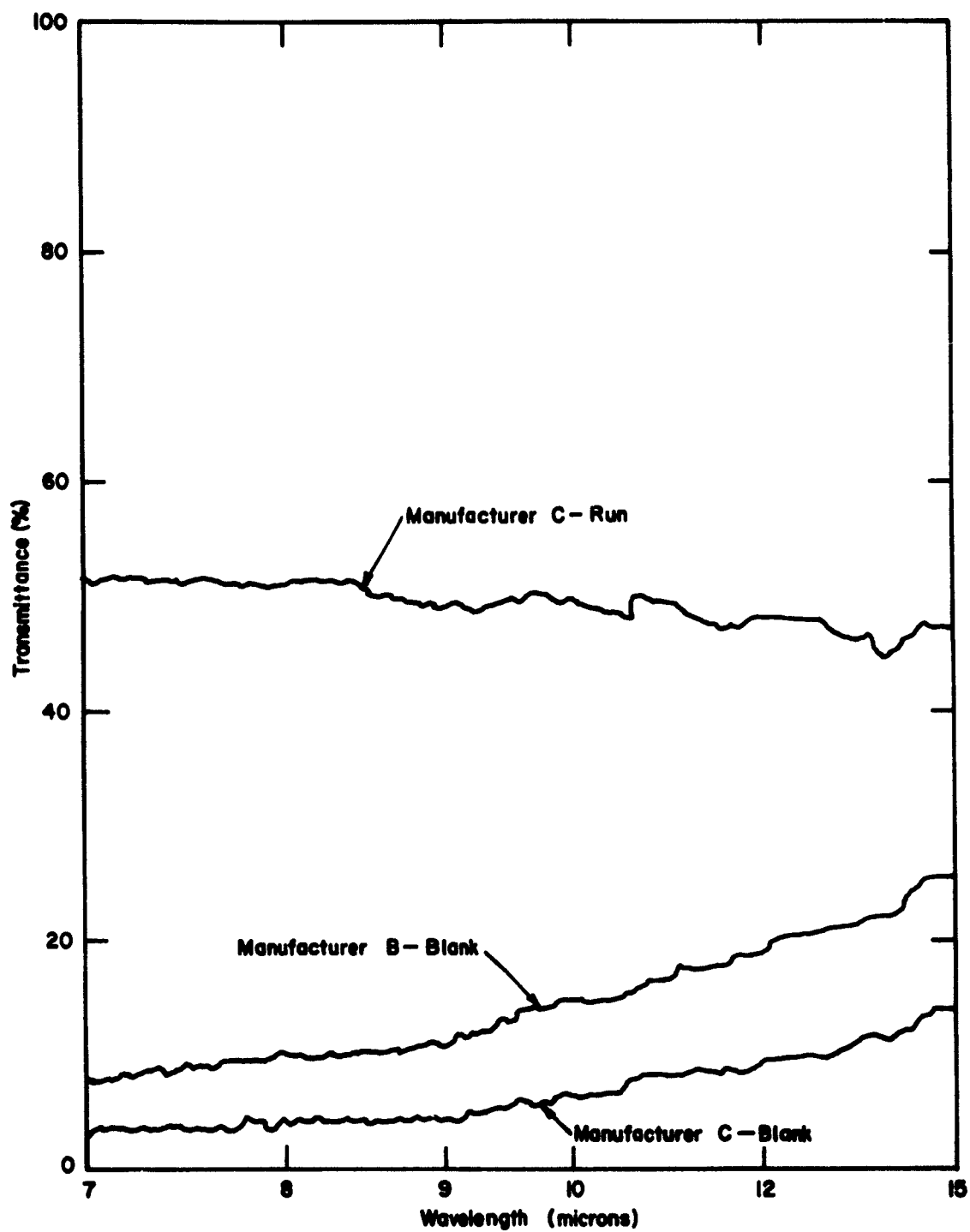
28

FIG. II   INFRARED MEASUREMENTS

Bemski[6] has suggested a model for radiation damage pinning in high oxygen content silicon. In this model a bond is broken between two Si atoms freeing two electrons for the formation of two Si - O bonds bridging the broken Si - Si bond. The oxygen is believed to occupy an interstitial position. It is possible for a vacancy produced during irradiation to move into the strained region around the oxygen atom and become "pinned" into position. Energetically this center behaves like a center at 0.16 ev below the conduction band. This level is present in oxygen containing silicon and is not present in oxygen-free material.[7]

When silicon is bombarded with electrons or ions it tends to become intrinsic after long irradiation. Upon annealing, it tends to revert to its original condition. The threshold for the annealing of the oxygen-pinned vacancies described above is approximately 300°C.[8] The threshold for improvement of solar cells made by ion implantation is also around 300°C and it is probable that the improvement occurs when the heat-treating temperature is high enough to anneal out oxygen-pinned vacancies. The bombarded surface layer at this point would revert from intrinsic to its original conducting state, thereby lowering cell internal series resistance and raising power output.

Since the oxygen-vacancy annealing effect occurs in the 300-400°C range, it is unlikely that this effect is related to the sudden improvement in cell response after heat treatment at 800°C. However, since cells are invariably poor if they have high oxygen content, the oxygen content effect appears to be overriding the higher temperature effect. This would suggest that the oxygen effect cannot be completely annealed out if enough oxygen is present initially.

Two solutions are possible:

(1)   Use low oxygen content silicon.

(2)   Implant at low temperatures (-195°C) where defect
        introduction rate is lower by an order of magnitude. [7]

4.4   LATTICE DAMAGE BY BOMBARDMENT

In order to directly investigate damage to the lattice due to the implanting process, reflection electron diffraction studies were made of some of the samples.   The samples used had the front surface parallel to the (100) plane and were cleaved to give a sharp edge.   Reflection diffraction patterns of the surface were obtained by directing the electron beam across this free edge. [*]   The history of the four samples studied is given in Table III.

Table III - Electron Diffraction Sample Chracteristics

Sample	History
A	Not implanted or annealed
B	Implanted with no annealing
C	Implanted with annealing at 250°C for 63 hours
D	Implanted with annealing at 800°C for 16 hours

The implantations on samples B, C and D were made with 1.5 Mev B^{11} ions.

---

[*] This work was performed at RCA Laboratories, Camden, N. J.

The results of these investigations are shown in Figs. 12 and 13. A transmission pattern of MgO (Fig. 12 - upper left) was used as a calibration standard representative of a polycrystalline specimen. Reflection electron diffraction patterns of the above samples are shown in the other seven plates.

On Plate A.[1], taken of an unbombarded specimen, well-defined Laué spots and Kikuchi lines are evident. These are characteristic of a perfect crystal in which the orientation of the atoms is accurate and which has a surface free of detectable contaminants.

The bright central spots visible in the calibration standard and in Plates B.[1], B.[2] and D.[2] can be attributed to inelastically scattered electrons. The diffuse background visible on all patterns results from electrons scattered from the amorphous surface oxide layer and from a portion of the inelastically scattered electrons from the crystal proper. The thickness of the amorphous oxide layer is approximately 300-500 $\overset{\bullet}{\text{A}}$.

Plates B.[1] and B.[2], from an implanted but non-heat-treated sample, show that the implantation destroys the characteristic single-crystal structure. There is evidence of a slight degree of residual crystallinity in both plates, but the surface has become almost amorphous.

Partial restoration of the crystal structure as the result of 250°C annealing is shown in Plates C.[1] and C.[2]. Complete restoration, within the sensitivity of the technique, in a sample annealed at 800°C is evident in Plates D.[1] and D.[2]. The patterns in the latter are as well defined as those of the unbombarded cell in Plate A.[1].
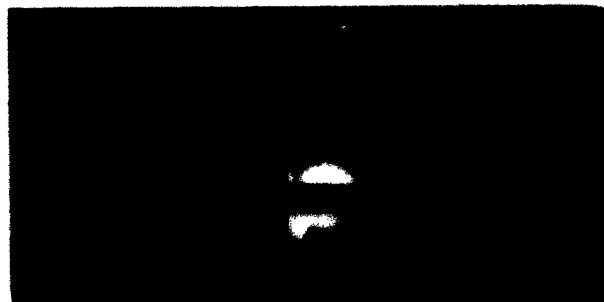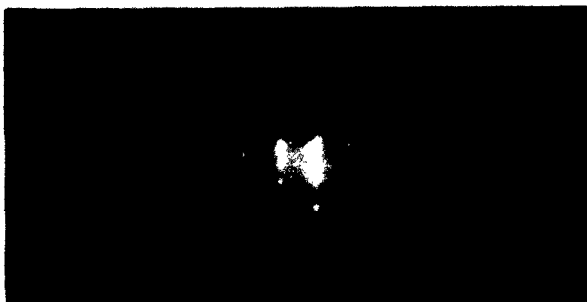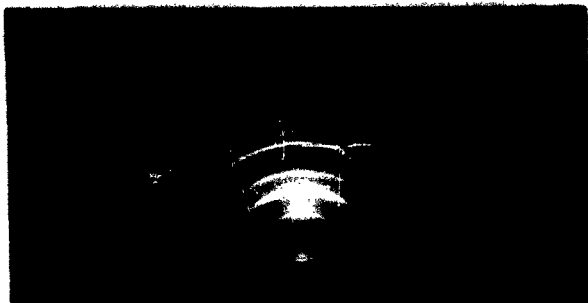
UPPER LEFT: CALIBRATION STANDARD   MgO

LOWER LEFT: PLATE A·[1]

UPPER RIGHT: PLATE B·[1]

LOWER RIGHT: PLATE B·[2]

UPPER LEFT: PLATE C.1

LOWER LEFT: PLATE C.2

UPPER RIGHT: PLATE D.1

LOWER RIGHT: PLATE D.2

Several authors[9,10,11] have reported on the damage produced in silicon due to bombardment with a variety of energetic particles. The destruction of the characteristic structure is caused primarily by collision displacements although there may be some lattice distortion from interstitial boron. No indication of the latter is obtained in finished efficient cells as shown by Plates D.[1] and D.[2].

The above results indicate that the radiation damage produced in the implantation process can be completely annealed out at temperatures low enough to have no effect on bulk lifetime. Radiation damage therefore does not appear to present a serious problem in producing p-n junctions by ion implantation.

5. N-ON-P CELLS

Preliminary investigations have been made on n-on-p cells. Two 0.4 ohm-cm p-type samples implanted with a 2 μamp - 1 Mev spectroscopically pure phosphorus ion beam showed a slight photo response upon removal from the machine. After heat treatment at 800°C for 16 hours, they gave photovoltages of 0.5 volts. This indicates conclusively that both n-on-p and p-on-n junctions can be formed by ion implantation techniques and obviates radiation damage as the mechanism for type conversion.

Further work is being done on the phosphorus ion source. Additional n-on-p cells conforming to the optimum parameters determined in the p-on-n study will be made at the end of the program.

6.   FUTURE PROGRAM

During the remaining two months of the contract, work will be concentrated in the following areas:

(1)   <u>Drift field and junction depth effects</u> - An effort will be made to optimize the spectral response under solar illumination by determining the correct combination of drift field and junction depth. This study will be made with the solar simulator as test light source and results will be compared with predicted values based on spectral response curves.

(2)   <u>Low temperature implantation techniques</u> - Implantation will be made at liquid nitrogen temperature to determine if less radiation damage is produced than at ambient temperature implantation.

(3)   <u>n-on-p-type cells</u> - Cells will be fabricated using the best parameters determined from the p-on-n cell study.

(4)   <u>Radiation damage resistance</u> - If time permits, the effects of radiation damage due to electrons and/or protons on finished cells will be studied.

7. REFERENCES

1. Northcliffe, L. C., Private Communication, Yale University, New Haven, Connecticut.

2. Powers, D., and Whaling, W., Phys. Rev. 126, 61, 1962.

3. Hoffman Electronics Corporation - Technical Documentary Report ASD-TDR-62-245, Electronic Technology Laboratory, Wright-Patterson Air Force Base, Ohio, Sept. 1962.

4. Pfister, J. C., and Baruch, P., Radiation Enhanced Diffusion, Kyoto Conference on Lattice Defects, Sept. 1962.

5. Kaiser, W., Keck, P. H., and Lange, C. F., Phys. Rev. 101, 1264, 1956.

6. Bemski, G., J. Appl. Phys. 30, 1195, 1959.

7. Wertheim, S. K., and Buchanan, D. N. C., J. Appl. Phys. 30, 1232, 1959.

8. Bemski, G., and Augustyniak, W., Phys. Rev. 108, 645, 1957.

9. Ohl, R. S., BSTJ 31, 104, 1952.

10. Gianola, U. F., J. Appl. Phys., 28, 868, 1957.

11. Brattain, W. H., and Pearson, G. L., Phys. Rev. 80, 846, 1950.